International Journal of Minerals, Metallurgy and Materials
Volume 28, Number 12, December 2021, Page 1917
https://doi.org/10.1007/s12613-020-2188-8

Multi-objective collaborative optimization of metallurgical properties of iron carbon agglomerates using response surface methodology

Ji-wei Bao[1,2,3], *Zheng-gen Liu*[1,2,3], *Man-sheng Chu*[4], *Dong Han*[1,2,3], *Lai-geng Cao*[1,2,3], *Jun Guo*[1,2,3], *and Zi-chuan Zhao*[1,2,3]

1) School of Metallurgy, Northeastern University, Shenyang 110819, China
2) Institute for Frontier Technologies of Low-carbon Steelmaking, Northeastern University, Shenyang 110819, China
3) Liaoning Province Engineering Research Center for Technologies of Low-Carbon Steelmaking, Northeastern University, Shenyang 110819, China
4) State Key Laboratory of Rolling and Automation, Northeastern University, Shenyang 110819, China
(Received: 30 July 2020; revised: 2 September 2020; accepted: 4 September 2020)

Abstract: Iron carbon agglomerates (ICA) are used to realize low-carbon blast furnace ironmaking. In this study, the central composite design based on response surface methodology was used to synergistically optimize the compressive strength, reactivity, and post-reaction strength of ICA. Results show that the iron ore addition ratio significantly influences the compressive strength, reactivity, and post-reaction strength of ICA. The iron ore addition ratio and carbonization temperature or the iron ore addition ratio and carbonization time exert significant interaction effects on the compressive strength and reactivity of ICA, but it has no interaction effects on the post-reaction strength of ICA. In addition, the optimal process parameters are as follows: iron ore addition ratio of 15.30wt%, carbonization temperature of 1000°C, and carbonization time of 4.27 h. The model prediction results of compressive strength, reactivity, and post-reaction strength are 4026 N, 55.03%, and 38.24%, respectively, which are close to the experimental results and further verify the accuracy and reliability of the models.

Keywords: iron carbon agglomerates; compressive strength; reactivity; post-reaction strength; multi-objective collaborative optimization; response surface methodology

1. Introduction

In recent years, the situation of global warming has become increasingly serious, and CO_2 emission reduction has become a common challenge faced by mankind. Fossil fuel combustion is the main source of CO_2 generation. China's CO_2 emissions from fossil fuel combustion reached 9.528 billion tons in 2018 [1]. As a large consumer of fossil fuels, the steel industry is a major contributor to CO_2 emission. Moreover, the CO_2 emissions and energy consumption of blast furnace (BF) ironmaking account for over 80% and 70% of the iron and steel industries, respectively [2–4]. Therefore, BF ironmaking is the key to reduce the energy consumption and CO_2 emission of the iron and steel industries [5]. Nowadays, the utilization of iron coke (or ferro coke or ICA) as an innovative technology for low-carbon BF ironmaking has attracted increasing attention. Iron coke is the co-carbonization product of iron ore and coals. Iron ore is reduced to metallic iron during carbonization, which catalyzes the gasification reaction of iron coke and greatly improves the reactivity of iron coke. Naito *et al.* [6–9] reported that the utilization of highly reactive coke is an effective countermeasure to achieve low-carbon BF by reducing the temperature of the thermal reserve zone. The difference between the actual and equilibrium concentrations of CO in BF gas is increased by lowering the temperature of the thermal reserve zone. As a result, the reduction driving force of iron oxide inside the BF is improved. Therefore, the utilization of highly reactive iron coke in BF can improve the reaction efficiency, decrease the fuel ratio, and reduce CO_2 emission [6–9]. However, the addition of iron ore as an inert material reduces the mechanical strength of iron coke, and an increase in the reactivity of iron coke inevitably decreases its post-reaction strength.

Nomura *et al.* [10] found that the drum index (DI_{15}^{150}) of iron coke decreases to 41.7% when 20wt% iron ore powder is added to the coals. The reactivity of iron coke increases significantly with the increase in iron ore powder addition ra-

Corresponding authors: Man-sheng Chu E-mail: chums@smm.neu.edu.cn; Zheng-gen Liu E-mail: liuzg@smm.neu.edu.cn
© University of Science and Technology Beijing 2021

tio, whereas the post-reaction strength decreases gradually. Anyashiki *et al.* [11] reported that the reactivity of ferro coke increases with the increase in iron ore ratio, whereas the drum index (DI_6^{150}) decreases gradually. Moreover, the drum index of ferro coke greatly decreases when the addition ratio of iron ore exceeds 30wt%. Wang *et al.* [12−13] conducted single-factor and orthogonal experiments to optimize the metallurgical properties of iron coke hot briquette (ICHB). They found that the reactivity of ICHB significantly increases as the iron ore ratio increases from 0wt% to 20wt%, whereas the compressive strength greatly decreases. The effects of various preparation parameters on the compressive strength of ICHB are in order of briquetting temperature, bituminous coal ratio, carbonization temperature, carbonization time, and iron ore addition ratio. The above research results generally indicate that the reactivity and strength of iron coke are hard to optimize simultaneously. Uchida *et al.* [14] developed a 3 dimension (3D) prediction model of the strength of ferro coke. This model uses micro X-ray computed tomography to analyze quantitatively the proportions of pore, pore wall, iron, and pore space surrounding the iron particles. Image-based modeling indicates that the wall thickness increases, stress concentration is relaxed, and the strength of ferro coke increases with increasing addition of hyper-coal. Nishioka *et al.* [15] developed a mathematical BF model to predict the gasification reactivity of ferro coke. The gasification degree of ferro coke in BF was calculated using the mathematical BF model, which agreed well with the experimental results. Shi *et al.* [16] established a prediction model for the strength of ferro coke through multiple linear regression analysis. The model revealed the influence law of various factors on the strength of ferro coke and determined the appropriate value of each factor.

As mentioned above, most of the studies used a single-factor method, and only a few used an orthogonal experiment. Moreover, the prediction models for the metallurgical properties of iron coke only reveal the influence law of various factors on a single metallurgical property. The interaction effects of various factors on various metallurgical properties and the collaborative optimization of various metallurgical properties have been rarely studied. Therefore, the description of parameters affecting the experimental results is insufficient. In recent years, response surface methodology (RSM) has been successfully applied to the parameter optimization of engineering problems [17−20], especially those affected by multiple factors. The central composite design (CCD) based on RSM is a commonly used experimental design [21−23]. Analysis of variance (ANOVA) can be effectively used to determine the significance and influence law of each parameter and their interaction effects on the responses [24−25]. Moreover, the best preparation parameters can be found through multi-objective collaborative optimization of various responses. However, the application of RSM to the collaborative optimization of metallurgical properties of iron coke has not been reported.

This paper proposes the preparation of ICA by using a coal tar pitch (CTP) binder through briquetting by roller and carbonizing. This study aims to optimize the preparation parameters of ICA by RSM. Quadratic models of compressive strength, reactivity, and post-reaction strength were established by CCD based on RSM with iron ore ratio, carbonization temperature, and carbonization time as independent variables. The multi-objective optimization of compressive strength, reactivity, and post-reaction strength was carried out using Design Expert (version 8.0.6, STAT-EASE Inc., Minneapolis, USA), and the optimal process parameters for preparing ICA were obtained.

2. Experimental

2.1. Experimental materials

For this investigation, one type of iron ore and four types of coals collected from a Chinese steel enterprise were used. The chemical composition of iron ore is listed in Table 1. The X-ray diffraction (XRD) patterns of iron ore are shown in Fig. 1. The main mineral phases of iron ore are Fe_3O_4, Fe_2O_3, and SiO_2. In terms of iron ore size, the particles with less than 75 μm accounted for approximately 80wt%. The characteristic analyses of the coals are listed in Table 2. Among them, coal A and coal B are caking coals with high volatile content and caking index, coal C is a weak caking coal, and coal D is a non-caking coal with high fixed carbon and low volatile matter. All coals were crushed and screened to less than 4 mm. In addition, CTP was used as the binder to prepare ICA. CTP is similar to coal in structure and properties, has a strong affinity with coal, and can well infiltrate coal particles. CTP must be broken to less than 1 mm to mix well with the raw material mixture.

Table 1. Chemical composition of iron ore wt%

TFe	FeO	CaO	SiO_2	MgO	Al_2O_3
65.36	21.86	0.17	6.35	0.45	0.45

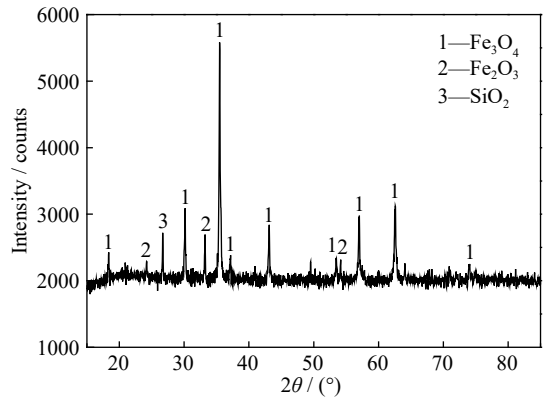

Fig. 1. XRD patterns of iron ore.

Table 2. Characteristic analyses of the coals (air dry basis)

Coal	Fixed carbon / wt%	Ash / wt%	Volatile matter / wt%	Gieseler fluidity			Caking index, *G* / %
				Initial softening temperature / °C	Temperature of maximum fluidity / °C	Curing temperature / °C	
A	61.21	8.96	29.08	440	476	498	74
B	69.84	10.74	19.10	430	472	495	75
C	76.50	9.90	13.16	n.a.	n.a.	n.a.	15
D	78.25	13.36	7.30	n.a.	n.a.	n.a.	n.a.

Note: n.a.—no data available.

2.2. Preparation of ICA

The preparation process of ICA is as follows: First, the iron ore and coals were dried at 105°C for 5 h in a blast drying oven, and then iron ore, coals, and binder were mixed at a certain ratio. The mixtures were quickly loaded into the roller briquetting equipment (Luoyang Kaizheng Environmental Protection Equipment Co., Ltd., KYS175 type, China) and heated while stirring. After heating to 60°C, the mixtures were pressed into briquettes under a linear pressure of 29.4 kN/cm. Finally, the briquettes were carbonized using an SX_2-8-13 type electric heating furnace developed by Shenyang Energy Saving Electric Furnace Factory, China. The briquettes were heated to different temperatures at a heating rate of 3°C/min, and a constant temperature was retained for different times. The carbonized products (ICA) were cooled in an inert atmosphere, and their metallurgical properties were tested.

In these experiments, the proportions of coals A, B, C, and D in blending coals were maintained at 64.28wt%, 14.29wt%, 14.29wt%, and 7.14wt%, respectively, and their addition ratios were equidistantly decreased with increasing proportion of iron ore. In addition, binder CTP was added at a fixed rate of 5wt% of the total mass of raw materials.

2.3. Determination of compressive strength of ICA

ICA should have good mechanical strength as a feed material for BF. Compressive strength is an important index of mechanical strength. The compressive strength of ICA was measured using an electronic universal testing machine (WDW-QT10 type). Twelve samples were randomly selected to measure the compressive strength, and the final experimental value is the average of the remaining results after removing the maximum and minimum.

2.4. Determination of reactivity and post-reaction strength of ICA

The reactivity and post-reaction strength of ICA were measured in accordance with GB/T 4000—2017 [26]. In N_2 atmosphere with a flow rate of 0.8 L/min, 200 g of ICA was heated to 1100°C at a rate of 10°C/min and then reacted with CO_2 (with a flow rate of 5 L/min) for 2 h at 1100°C. After the reaction, the post-reaction strength of ICA was performed by 600 revolutions (20r/min × 30 min) in an I-type drum (ϕ130 mm × 700 mm). After the drum test, the samples were screened with a 10 mm round hole sieve, and the quality of the material on the sieve was recorded. The reactivity index (RI) of ICA was evaluated by calculating the carbon conversion ratio using Eq. (1).

$$\mathrm{RI} = \frac{m_0 \times c_0 - m_1 \times c_1}{m_0 \times c_0} \times 100\% \quad (1)$$

where m_0 and m_1 are the mass of ICA before and after reaction, respectively, g; c_0 is the carbon content of ICA before the reaction, and c_1 is the carbon content of ICA after the reaction.

The post-reaction strength (PRS) of ICA was estimated by the percentage of the mass of reacted ICA with a particle size greater than 10 mm after the drum test to the mass of reacted ICA, as shown in Eq. (2):

$$\mathrm{PRS} = \frac{m_2}{m_1} \times 100\% \quad (2)$$

where m_2 is the mass of reacted ICA with particle sizes larger than 10 mm after the drum test, g.

2.5. Characterization methods

The microstructure of ICA prepared under the optimized conditions was analyzed using scanning electron microscopy–energy dispersive X-ray spectroscopy (SEM–EDS, Zeiss, Ultra Plus, Germany). The samples were cut, and then the cut samples without mounting processing were ground using different grades of sandpaper and polished by a polishing machine. Finally, the sample surface was coated with gold-palladium alloy for SEM–EDS. In addition, the mineral phase composition of ICA prepared under the optimized conditions was analyzed through XRD (Panalytical B.V., MPDDY2094 type, the Netherlands) with Cu K_α radiation. The scanning range for the XRD analysis was from 10° to 90° at a scanning rate of 0.2°/s.

2.6. Design of experiment by RSM

RSM is an experimental design and optimization method through modeling with the help of mathematical and statistical techniques. It uses regression to fit the function relation between each factor and the results in the global scope through local test on specific points. Therefore, the influence of each factor and their interaction effects on the results can be quantitatively analyzed, and the optimal level of each

factor can be obtained. For most industrial problems, a second-order polynomial regression model can be established through RSM for analysis, which is given by Eq. (3) [27−28]:

$$Y = \beta_0 + \sum_{i=1}^{k}\beta_i x_i + \sum_{i=1}^{k}\beta_{ii}x_i^2 + \sum_{i=1}^{k-1}\sum_{j=i+1}^{k}\beta_{ij}x_i x_j + \varepsilon \quad (3)$$

where Y is the response predicted by the model; x_i and x_j are the independent variables; β_0, β_i, β_{ii}, and β_{ij} are the constant, linear, quadratic, and interaction coefficients, respectively; k is the number of factors; ε is the random error.

The CCD of RSM can be used to study the influence of single variable and multiple variable interactions on the response [21−22]. In this study, a CCD with three variables and five levels was used for experimental design to investigate the effects of iron ore addition ratio, carbonization temperature, and carbonization time on the compressive strength, reactivity, and post-reaction strength of ICA. The five levels of the three variables are listed in Table 3. The levels of three independent variables were chosen on the basis of the authors' previous studies. In general, the catalytic activation of ICA using iron ore was carried out in the range of 5wt%–40wt%. In addition, the temperature and time for the conversion of coals to mature coke determine the range of carbonization temperature and carbonization time, which are 800–1200°C and 2–6 h, respectively. The experimental design matrix generated using Design Expert is shown in Table 4. It includes 20 experimental points (eight factorial points, six axial points, and six center points), and all combinations of independent variables are included. The detailed experimental conditions and the corresponding experimental results are listed in Table 4.

Table 3. Values and levels of the independent variables used in the CCD

Independent variable	Symbol	Range and level				
		−1.68179	−1	0	1	1.68179
Iron ore addition ratio / wt%	x_1	3.18	10	20	30	36.82
Carbonization temperature / °C	x_2	831.82	900	1000	1100	1168.18
Carbonization time / h	x_3	2.32	3	4	5	5.68

Table 4. Experimental design matrix and results for CCD

Run	Iron ore addition ratio, x_1 / wt%	Carbonization temperature, x_2 / °C	Carbonization time, x_3 / h	Compressive strength, Y_1 / N	Reactivity, Y_2 / %	Post-reaction strength, Y_3 / %
1	10	900	3	4249	50.56	62.99
2	30	900	3	3001	68.26	12.25
3	10	1100	3	3926	52.05	58.99
4	30	1100	3	3162	59.56	10.55
5	10	900	5	4002	53.36	64.13
6	30	900	5	2967	65.21	11.40
7	10	1100	5	3894	52.15	62.13
8	30	1100	5	2964	58.45	10.26
9	3.18	1000	4	4244	50.54	76.09
10	36.82	1000	4	2424	66.00	6.56
11	20	831.82	4	3598	56.76	22.23
12	20	1168.18	4	3971	53.13	24.22
13	20	1000	2.32	3402	56.70	18.81
14	20	1000	5.68	3697	53.98	26.37
15	20	1000	4	3922	60.42	25.65
16	20	1000	4	3670	54.80	30.21
17	20	1000	4	3832	57.21	20.81
18	20	1000	4	3948	57.14	27.65
19	20	1000	4	3663	57.26	24.80
20	20	1000	4	3954	57.37	23.37

3. Results and discussion

3.1. Model fitting

The linear model, two factor interaction model (2FI), and quadratic model were used to conduct regression fitting of the experimental data in Table 4. The simulated results are listed in Table 5.

For the regression fitting of experimental data, the R^2 and

Table 5. Statistics summary of simulated results

Source	Compressive strength / N			Reactivity / %			Post-reaction strength / %		
	Standard deviation	R^2	Adjusted R^2	Standard deviation	R^2	Adjusted R^2	Standard deviation	R^2	Adjusted R^2
Linear	234.53	0.8051	0.7686	2.26	0.8266	0.7940	8.18	0.8759	0.8527
2FI	253.60	0.8149	0.7294	1.84	0.9060	0.8626	9.05	0.8766	0.8197
Quadratic	162.03	0.9419	0.8895	1.74	0.9355	0.8775	5.68	0.9626	0.9290

adjusted R^2 of the quadratic model are the largest among the three models. This result indicates that the regression fitting result of the quadratic model is the best. The adjusted R^2 values for the quadratic models of compressive strength, reactivity, and post-reaction strength are 0.8895, 0.8775, and 0.9290, respectively, and the R^2 values for the quadratic models of compressive strength, reactivity, and post-reaction strength are 0.9419, 0.9355, and 0.9626, respectively. This result indicates a high correlation between the actual and predicted values. Therefore, the quadratic model is selected to conduct regression fitting of the experimental data. Similar to Eq. (3), second-order quadratic models of the compressive strength, reactivity, and post-reaction strength of ICA were established as follows.

For compressive strength:

$$Y_1 = 1949.08363 - 55.57609x_1 + 2.64301x_2 + 752.53448x_3 + 0.73625\times10^{-1}x_1x_2 + 0.58750x_1x_3 + 0.06375x_2x_3 - 1.79831x_1^2 - 2.05554\times10^{-3}x_2^2 - 103.64042x_3^2 \quad (4)$$

For reactivity:

$$Y_2 = -47.70701 + 2.58780x_1 + 0.14239x_2 + 5.76349x_3 - 0.19675\times10^{-2}x_1x_2 - 0.08825x_1x_3 - 0.00095x_2x_3 + 6.01448\times10^{-3}x_1^2 - 5.74117\times10^{-5}x_2^2 - 0.43446x_3^2 \quad (5)$$

For post-reaction strength:

$$Y_3 = 201.39490 - 5.33782x_1 - 0.17910x_2 - 5.05943x_3 + 3.91875\times10^{-4}x_1x_2 - 0.67687\times10^{-1}x_1x_3 + 3.20625\times10^{-3}x_2x_3 + 0.71706\times10^{-1}x_1^2 + 7.72131\times10^{-5}x_2^2 + 0.54586x_3^2 \quad (6)$$

where Y_1, Y_2, and Y_3 are the compressive strength, reactivity, and post-reaction strength of ICA, respectively, and codes x_1, x_2, and x_3 are the iron ore addition ratio, carbonization temperature, and carbonization time, respectively.

3.2. ANOVA and evaluation of the fitted models

ANOVA was used to investigate the accuracy and significance of the quadratic models, and the results are listed in Tables 6–8. *F*-value is the ratio of mean square between groups (MS_b) to mean square within groups (MS_w), and *P*-value refers to the probability value of corresponding *F*-value. The significance of each model item is tested by *P*-value and *F*-value. The larger the *F*-value and the smaller the *P*-value are, the more significant the corresponding model item is. *P*-value < 0.01 indicates that the influence of the model item is extremely significant, *P*-value < 0.05 indicates that the influence of the model item is significant, and *P*-value > 0.05 indicates that the influence of the model item is not significant. For the overall model, *P*-value < 0.01 is found in the designed models of compressive strength, reactivity, and post-reaction strength, which indicates that the quadratic models selected in this experiment have high accuracy, good fitting, and statistical significance. For lack of fit, the *P*-values of the three quadratic models are 0.2530, 0.5484, and 0.0512, respectively, which indicates that the quadratic models selected have no significant relative pure error and have good adaptability and high fitting precision. For the responses of the three quadratic models, the predicted R^2 values are close to the adjusted R^2 values, and the differences between them are close to or less than 0.2. The adequate precision indicates a measure of the "signal-to-noise ratio" and the measurement method with "signal-to-noise ratio" greater than 4 has sufficient accuracy and is considered reasonable. The adequate precision values of the three responses are 15.129, 13.886, and 19.674, confirming that the current models can be used to navigate the design space.

In the linear term, the influence of x_1 on the compressive strength of ICA is extremely significant. In the quadratic term, the influences of x_1^2 and x_3^2 are significant, whereas that of x_2^2 is not significant. Therefore, the influences of the different parameters on the compressive strength of ICA are in the order of iron ore addition ratio > carbonization time > carbonization temperature. For the reactivity of ICA, the influences of x_1 and x_2 in the linear term are extremely significant, whereas the influence of x_3 is not significant. In the interaction term, the influence of x_1x_2 is extremely significant, whereas the influences of x_1x_3 and x_2x_3 are not significant. Therefore, the influences of the parameters on the reactivity of ICA are in the order of iron ore addition ratio > carbonization temperature > carbonization time. For the post-reaction strength of ICA, the influence of x_1 in the linear term is extremely significant, whereas the influences of x_2 and x_3 are

Table 6. ANOVA results for the quadratic model of compressive strength

Source	Sum of squares	Degree of freedom	Mean square	*F*-value	*P*-value	Status
Model	4.254×10^6	9	4.726×10^5	18.00	<0.0001	Extremely significant
x_1	3.627×10^6	1	3.627×10^6	138.14	<0.0001	Extremely significant
x_2	9192.06	1	9192.06	0.35	0.5672	Not significant
x_3	16.19	1	16.19	6.168×10^{-4}	0.9807	Not significant
x_1x_2	43365.13	1	43365.13	1.65	0.2277	Not significant
x_1x_3	276.13	1	276.13	0.011	0.9203	Not significant
x_2x_3	325.13	1	325.13	0.012	0.9136	Not significant
x_1^2	4.661×10^5	1	4.661×10^5	17.75	0.0018	Extremely significant
x_2^2	6089.11	1	6089.11	0.23	0.6405	Not significant
x_3^2	1.548×10^5	1	1.548×10^5	5.90	0.0356	Significant
Residual	2.625×10^5	10	26254.09			
Lack of fit	1.713×10^5	5	34259.49	1.88	0.2530	Not significant
Pure error	91243.50	5	18248.70			
Total	4.516×10^6	19				

Adj. R^2 = 0.8895; Pred. R^2 = 0.6765; Adeq. precision = 15.129.

Table 7. ANOVA results for the quadratic model of reactivity

Source	Sum of squares	Degree of freedom	Mean square	*F*-value	*P*-value	Status
Model	439.07	9	48.79	16.12	<0.0001	Extremely Significant
x_1	352.27	1	352.27	116.38	<0.0001	Extremely Significant
x_2	33.17	1	33.17	10.96	0.0079	Extremely Significant
x_3	2.49	1	2.49	0.82	0.3855	Not significant
x_1x_2	30.97	1	30.97	10.23	0.0095	Extremely Significant
x_1x_3	6.23	1	6.23	2.06	0.1819	Not significant
x_2x_3	0.072	1	0.072	0.024	0.8803	Not significant
x_1^2	5.21	1	5.21	1.72	0.2187	Not significant
x_2^2	4.75	1	4.75	1.57	0.2388	Not significant
x_3^2	2.72	1	2.72	0.90	0.3655	Not significant
Residual	30.27	10	3.03			
Lack of fit	14.27	5	2.85	0.89	0.5484	Not significant
Pure Error	16.00	5	3.20			
Total	469.34	19				

Adj. R^2 = 0.8775; Pred. R^2 = 0.7116; Adeq. precision = 13.886.

Table 8. ANOVA results for the quadratic model of post-reaction strength

Source	Sum of squares	Degree of freedom	Mean square	*F*-value	*P*-value	Status
Model	8299.93	9	922.21	28.60	<0.0001	Extremely significant
x_1	7532.17	1	7532.17	233.61	<0.0001	Extremely significant
x_2	2.20	1	2.20	0.068	0.7993	Not significant
x_3	18.37	1	18.37	0.57	0.4677	Not significant
x_1x_2	1.23	1	1.23	0.038	0.8491	Not significant
x_1x_3	3.67	1	3.67	0.11	0.7430	Not significant
x_2x_3	0.82	1	0.82	0.026	0.8763	Not significant
x_1^2	740.99	1	740.99	22.98	0.0007	Extremely significant
x_2^2	8.59	1	8.59	0.27	0.6169	Not significant
x_3^2	4.29	1	4.29	0.13	0.7228	Not significant
Residual	322.42	10	32.24			
Lack of fit	268.58	5	53.72	4.99	0.0512	Not significant
Pure Error	53.84	5	10.77			
Total	8622.35	19				

Adj. R^2 = 0.9290; Pred. R^2 = 0.7553; Adeq. precision = 19.674.

not significant. In the quadratic term, x_1^2 has an extremely significant effect, whereas x_2^2 and x_3^2 have no significant effect. Therefore, the iron ore addition ratio exerts the most significant effect on the post-reaction strength of ICA, whereas the carbonization temperature and carbonization time exert no significant effect.

Fig. 2 shows the normal probability distributions of residuals for the compressive strength, reactivity, and post-reaction strength models. The residual scatters of the three models are almost distributed on a straight line, which indicates that the errors are normally distributed and the fitting effects of the three models are extremely good [29−30]. The comparison between the predicted and actual values of the compressive strength, reactivity, and post-reaction strength models is shown in Fig. 3. The scatters of the actual and predicted values are approximately distributed on a straight line, indicating that the actual and predicted values have a high degree of fit. On the basis of the above analysis, the prediction models of compressive strength, reactivity, and post-reaction strength established by RSM are reliable.

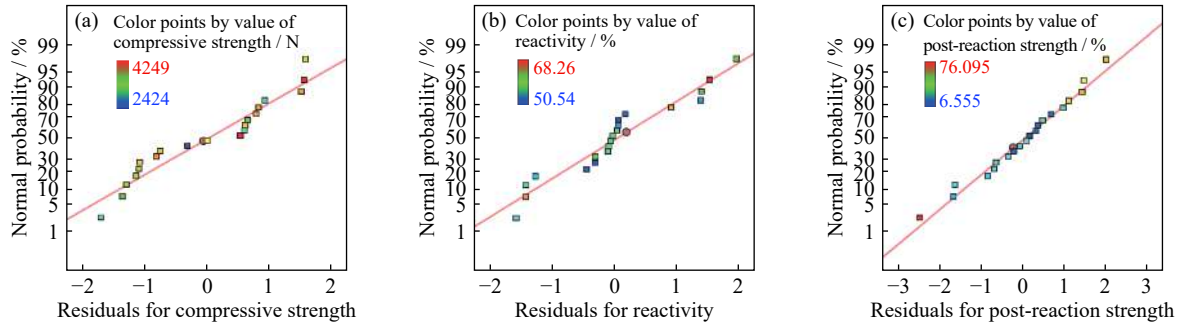

Fig. 2. Normal probability distribution of residuals for (a) compressive strength, (b) reactivity, and (c) post-reaction strength.

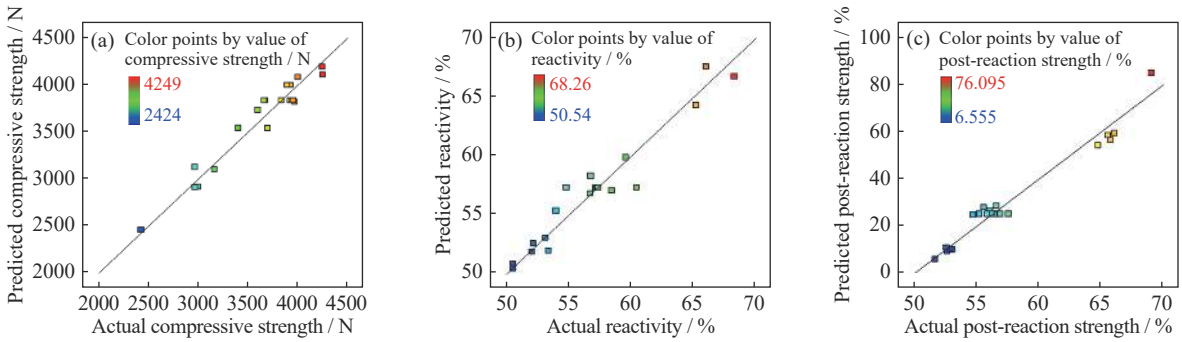

Fig. 3. Comparison between predicted and actual values for (a) compressive strength, (b) reactivity, and (c) post-reaction strength.

3.3. Effects of preparation variables on the metallurgical properties of ICA

3.3.1. Effects of preparation variables on the compressive strength of ICA

The interaction effects of iron ore addition ratio and carbonization temperature on the compressive strength of ICA were studied at a carbonization time of 4 h through 3D response surface plots, as shown in Fig. 4(a). The compressive strength of ICA decreases significantly as the iron ore addition ratio is increased from 10wt% to 30wt%. Meanwhile, as the carbonization temperature is increased from 900 to 1100°C, the compressive strength of ICA initially increases slowly and then flattens out. Moreover, the effect of iron ore addition ratio is more significant than that of carbonization temperature. This result is confirmed by the lower *P*-value of iron ore addition ratio than that of carbonization temperature in Table 6. The steepness of the response surface in Fig. 4(a) suggests that the steepness of the iron ore addition ratio direction is greater than that of the carbonization temperature, which can also confirm the above result.

Fig. 4(b) shows the interaction effect of iron ore addition ratio and carbonization time on the compressive strength at a carbonization temperature of 1000°C. Similar to the effect of carbonization temperature on compressive strength, the compressive strength initially increases slowly and then flattens out with the extension of carbonization time. Compared with the carbonization time, the iron ore addition ratio exerts a more significant influence on compressive strength. This result is also proven by the relatively lower *P*-value of iron ore addition ratio and the steeper curves in the direction of iron ore addition ratio. The interaction effect of carbonization temperature and carbonization time on the compressive strength at an iron ore addition ratio of 20wt% is shown in Fig. 4(c). The response surface slope is flat, and the interaction effect of carbonization temperature and carbonization time on compressive strength is not significant. However, the

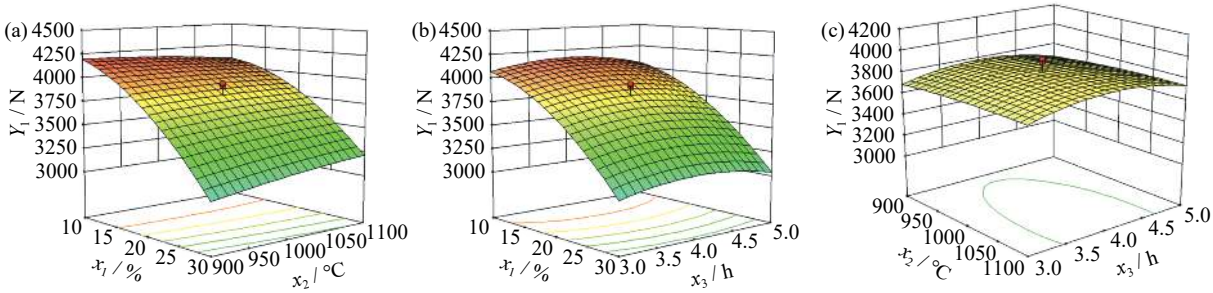

Fig. 4. 3D response surface plots for effects of iron ore ratio (x_1), carbonization temperature (x_2), and carbonization time (x_3) on compressive strength (Y_1): (a) x_1 and x_2; (b) x_1 and x_3; (c) x_2 and x_3.

direction of carbonization time is steeper, and the effect of carbonization time is more significant than that of carbonization temperature.

3.3.2. Effects of preparation variables on reactivity of ICA

At a carbonization time of 4 h, the interaction effect of iron ore addition ratio and carbonization temperature on the reactivity of ICA is shown in Fig. 5(a). As the iron ore addition ratio is increased from 10wt% to 30wt%, the reactivity of ICA is significantly improved. However, the reactivity of ICA decreases significantly with the increase in carbonization temperature from 900 to 1100°C. In Table 7, the low *P*-values of iron ore addition ratio, carbonization temperature, and the interaction between iron ore addition ratio and carbonization temperature indicate that the iron ore addition ratio and the carbonization temperature exert significant influences on reactivity, and their interaction effect is also significant. Meanwhile, the response surface in the direction of iron ore addition ratio is steeper, and the iron ore addition ratio exerts a greater effect on the reactivity of ICA compared with the carbonization temperature.

The interaction effect of iron ore addition ratio and carbonization time on the reactivity at a carbonization temperature of 1000°C is shown in Fig. 5(b). The reactivity of ICA decreases slightly with the extension of carbonization time. These data indicate that the carbonization time exerts less significant influence on reactivity than the iron ore addition ratio, as evidenced by the relatively larger *P*-value of carbonization time and the flatter curve in the direction of carbonization time. Fig. 5(c) shows the interaction effect of carbonization temperature and carbonization time on the reactivity of ICA at an iron ore addition ratio of 20wt%. The response surface slope is flat, and the interaction effect of carbonization temperature and carbonization time on the reactivity of ICA is not significant. However, the steepness of the carbonization temperature direction is greater, and the influence of carbonization temperature on the reactivity of ICA is greater than that of carbonization time.

3.3.3. Effects of preparation variables on post-reaction strength of ICA

Figs. 6(a) and 6(b) show the interaction effects of iron ore addition ratio and carbonization temperature, iron ore addition ratio and carbonization time on the post-reaction strength of ICA, respectively. The post-reaction strength of ICA decreases significantly with the increase in iron ore addition ratio. However, the carbonization temperature and carbonization time exert no significant effect on the post-reaction strength of ICA. In addition, the steepness of the response surface is greater in the direction of iron ore addition ratio. Therefore, the effect of iron ore addition ratio on the post-reaction strength is more significant than those of carbonization temperature and carbonization time. The interaction effect of carbonization temperature and carbonization time on the post-reaction strength of ICA is shown in Fig. 6(c). The slope of response surface is gentle, which indicates that the carbonization temperature and carbonization time exert minimal influence on the response. Therefore, carbonization temperature and carbonization time are not the main factors

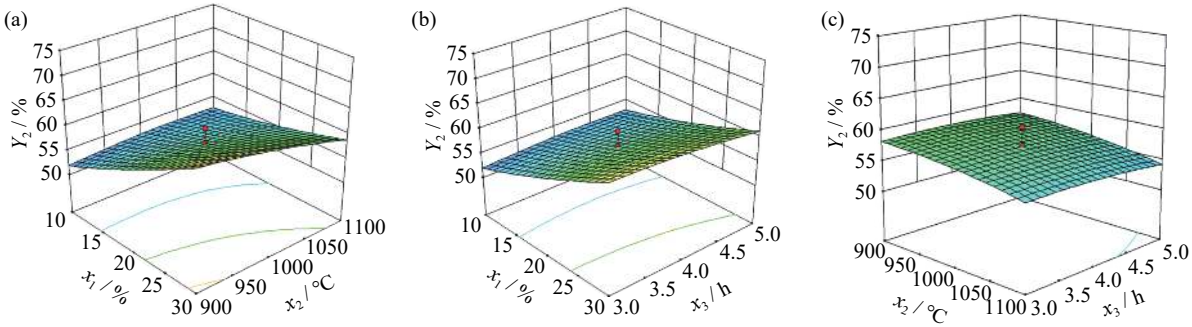

Fig. 5. 3D response surface plots for effects of iron ore ratio (x_1), carbonization temperature (x_2), and carbonization time (x_3) on the reactivity (Y_2): (a) x_1 and x_2; (b) x_1 and x_3; (c) x_2 and x_3.

affecting the post-reaction strength of ICA.

The above analysis suggests that increasing the iron ore addition ratio can improve the reactivity of ICA but reduce the compressive strength and post-reaction strength of ICA. Increasing the carbonization temperature and carbonization time can improve the compressive strength and reduce the reactivity of ICA. However, the influence of carbonization temperature and carbonization time is not significant relative to that of iron ore addition ratio. Therefore, with comprehensive consideration of economic costs, the carbonization temperature and carbonization time should be increased as much as possible to improve the compressive strength of ICA. At the same time, on the premise of reducing the decrease of compressive strength and post-reaction strength of ICA caused by iron ore addition, the iron ore addition ratio should be increased as much as possible to improve the reactivity of ICA.

3.4. Multi-objective collaborative optimization and experimental verification

High product quality, including high compressive strength, reactivity, and post-reaction strength, is required to use ICA in industrial production. However, multi-objective optimization is difficult to achieve during the preparation of ICA. Accordingly, three objective functions (compressive strength (Y_1), reactivity (Y_2), and post-reaction strength (Y_3)) were considered in this study to optimize the desired function for multiple objectives. The design variable optimization objectives of iron ore addition ratio, carbonization temperature, and carbonization time were set within the "in range." In addition, the optimization goals were set to the maximum responses to obtain the maximum compressive strength, reactivity, and post-reaction strength. The optimization tool of Design Expert software was used for collaborative optimization of the three objectives. The optimization constraints adopted in this study are shown in Table 9.

The final optimal parameters are as follows: iron ore addition ratio of 15.30wt%, carbonization temperature of 1000°C, and carbonization time of 4.27 h. Under the optimized conditions, the predicted results by the model are a compressive strength of 4026 N, a reactivity of 55.03%, and a post-reaction strength of 38.24%. The preparation experiments of ICA were carried out under optimal conditions to verify the optimized results. The results are shown in Table 10. The experimental results of compressive strength, reactivity, and post-reaction strength are 3996 N, 52.16%, and 40.10%, respectively, which are close to the predicted results of model optimization, and the errors are only 0.74%, 5.22%, and 4.86%, respectively. The results show that the multi-objective optimal process parameters obtained by Design Expert are accurate enough and the predictions of the three models are reliable.

3.5. Characterization of ICA prepared under optimized conditions

XRD analysis showed that the iron ore mainly consists of Fe_3O_4, Fe_2O_3, and SiO_2 (Fig. 1). XRD patterns of ICA prepared under the optimized process conditions are shown in Fig. 7. The main mineral phases of ICA are Fe, Fe_3O_4, and SiO_2. Fe_3O_4 and Fe_2O_3 are almost reduced to Fe in the carbonization process. The metal iron (Fe) could play a catalytic role in the gasification reaction between ICA and CO_2. The section of ICA prepared under optimized conditions was observed by SEM, as shown in Fig. 8. The results of EDS show

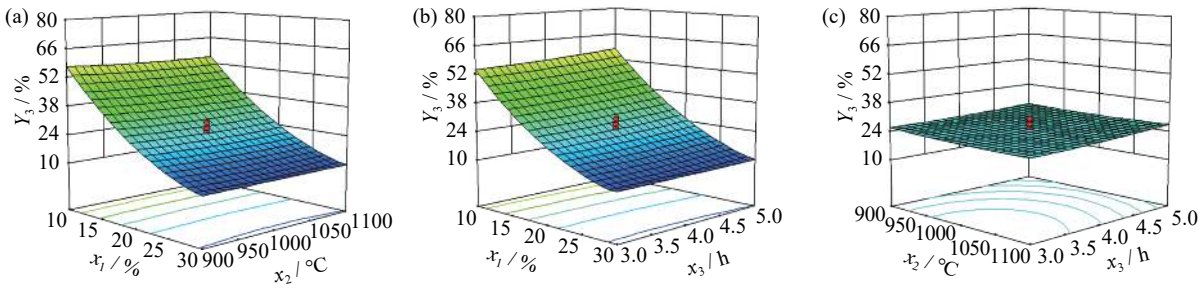

Fig. 6. 3D response surface plots for effects of iron ore ratio (x_1), carbonization temperature (x_2), and carbonization time (x_3) on the post-reaction strength (Y_3): (a) x_1 and x_2; (b) x_1 and x_3; (c) x_2 and x_3.

Table 9. Optimization constraints

Parameter	Goal	Lower limit	Upper limit	Importance
Iron ore ratio, x_1 / %	In range	10	40	3
Carbonization temperature, x_2 / °C	In range	1000	1200	3
Carbonization time, x_3 / h	In range	3	6	3
Compressive strength, Y_1 / N	Maximize	3500	4300	5
Reactivity, Y_2 / %	Maximize	55	70	5
Post-reaction strength, Y_3 / %	Maximize	38	80	5

Table 10. Predicted and experimental results under optimal conditions

Parameter	Predicted results	Experimental results	Error / %
Iron ore ratio, x_1 / %	15.30	15.00	1.96
Carbonization temperature, x_2 / ℃	1000	1000	0
Carbonization time, x_3 / h	4.27	4	6.32
Compressive strength, Y_1 / N	4026	3996	0.74
Reactivity, Y_2 / %	55.03	52.16	5.22
Post-reaction strength, Y_3 / %	38.24	40.10	4.86

that the dark gray area is C, the white area is Fe, and the light gray area is SiO_2, which is consistent with the results of XRD analysis, and most of iron oxides are reduced to metallic iron. Moreover, the metal iron is evenly distributed in the carbon matrix, and the metal iron closely combined with the carbon matrix can form active sites, which play a catalytic role in the gasification reaction between the carbon matrix and CO_2, and greatly improve the reactivity of ICA. In addition, the microstructure of ICA is highly dense with small pores and low porosity, which is highly conducive to improving the mechanical strength of ICA. The proximate analysis of ICA prepared under optimized conditions is listed in Table 11.

ICA with high reactivity and high strength was prepared by synergistically optimizing its compressive strength, reactivity, and post-reaction strength. The compressive strength of ICA prepared under optimized conditions is 3996 N, which is much higher than the 2000 N required by usual metallurgical cokes [31]. According to the Chinese metallurgical coke standard GB/T 1996—2017 [32], the reactivity and post-reaction strength of secondary metallurgical coke are ≤35% and ≥55%, respectively. The reactivity and post-reaction strength of ICA prepared under optimized conditions are 52.16% and 40.1%, respectively. As a new type of burden,

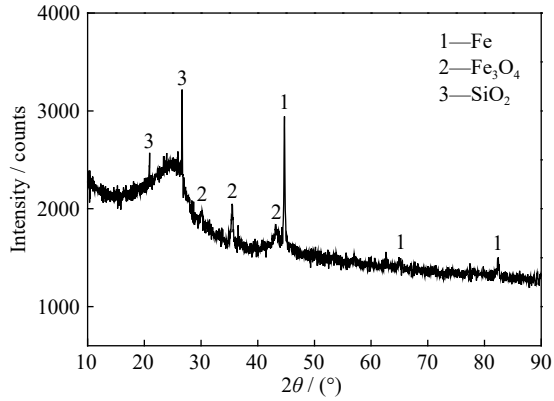

Fig. 7. XRD pattern of ICA prepared under optimized conditions.

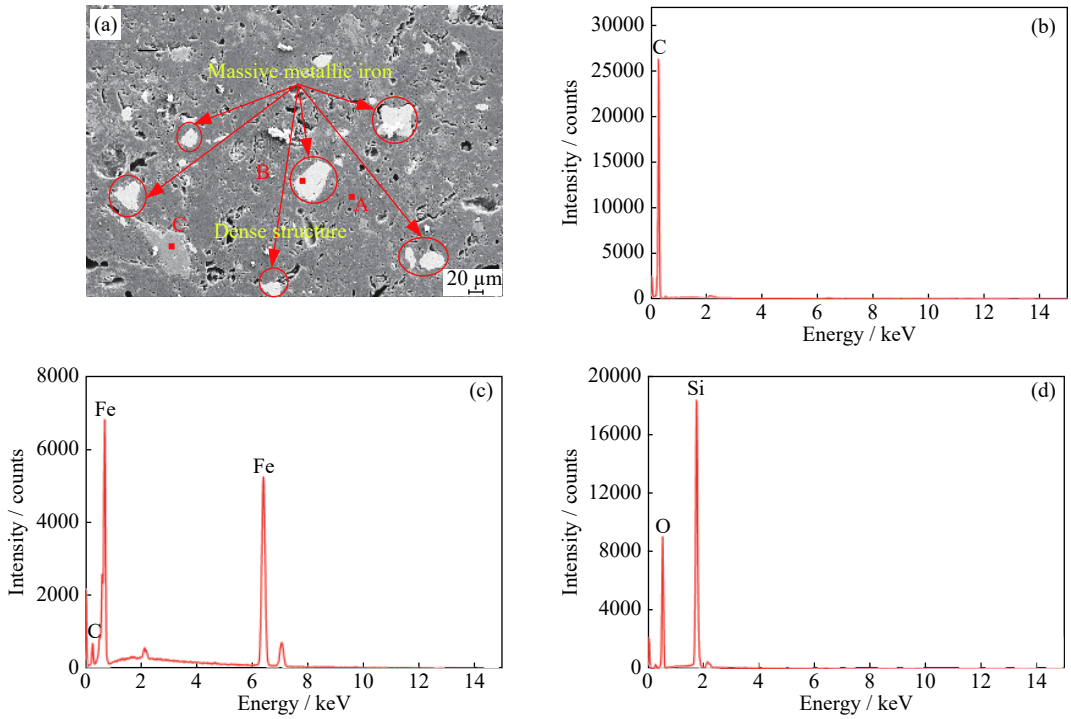

Fig. 8. SEM–EDS analysis of ICA prepared under optimized conditions: (a) cross section; (b) EDS spectrum of point A; (c) EDS spectrum of point B; (d) EDS spectrum of point C.

Table 11. Proximate analysis of ICA prepared under optimized conditions (air dry basis) wt%

Fixed carbon	Ash	Volatile matter	Moisture
66.91	28.95	1.88	2.26

ICA only replaces part of coke in BF, but does not replace the skeleton role of coke. The high reactivity of ICA is mainly used to preferentially react with CO_2 to protect coke, and it can reduce the temperature of thermal reserve zone and promote the reduction of iron bearing burden. Therefore, ICA cannot be simply measured by metallurgical coke standard. Meanwhile, the reactivity of ICA is much higher than that of metallurgical coke, which embodies the value of its low-carbon BF smelting. The post-reaction strength of ICA is close to the requirement of secondary metallurgical coke. On the basis of greatly optimized reactivity, the post-reaction strength has been greatly improved. The above research is of great significance and will provide guidance for the industrial production and BF application of ICA.

4. Conclusions

(1) Quadratic models of compressive strength, reactivity, and post-reaction strength of ICA were established successfully by RSM. The significant influence parameters of the quadratic models were determined by ANOVA, and the accuracy of the models was also illustrated.

(2) The iron ore addition ratio and carbonization temperature or the iron ore addition ratio and carbonization time exerted significant interaction effects on the compressive strength and reactivity of ICA. However, no obvious interaction was found between the carbonization temperature and carbonization time. The influence of the parameters on the compressive strength is in the order of iron ore addition ratio > carbonization time > carbonization temperature, and the impact of the parameters on the reactivity is the order of iron ore addition ratio > carbonization temperature > carbonization time. The iron ore addition ratio has the most obvious influence on the post-reaction strength, whereas the effects of carbonization temperature and carbonization time are not significant, and the three variables do not interact with each other.

(3) The optimum parameters are iron ore addition ratio of 15.30wt%, carbonization temperature of 1000°C and carbonization time of 4.27 h through multi-objective collaborative optimization, and the model prediction results of compressive strength, reactivity, and post-reaction strength are 4026 N, 55.03%, and 38.24%, respectively. These values are close to the experimental results and further verify the accuracy and reliability of the models.

(4) The metal iron is evenly distributed in the carbon matrix of ICA prepared under optimized conditions, which can form active sites to catalyze the gasification reaction between ICA and CO_2. The microstructure of ICA prepared under optimized conditions is highly dense with small pores and low porosity, which can greatly improve the mechanical strength of ICA.

Acknowledgements

This work was financially supported by the National Natural Science Foundation of China-Liaoning Joint Funds (No. U1808212), the National Natural Science Foundation of China (No. 52074080), the Fundamental Research Funds of the Central Universities of China (No. N182504010), and Xingliao Talent Plan (No. XLYC1902118).

References

[1] IEA(2020), CO_2 Emissions from Fuel Combustion [2021-02-15]. https://www.iea.org/statistics/topics/CO2emissions

[2] H.T. Wang, M.S. Chu, W. Zhao, Z.G. Liu, and J. Tang, Influence of iron ore addition on metallurgical reaction behavior of iron coke hot briquette, *Metall. Mater. Trans. B*, 50(2019), No. 1, p. 324.

[3] Z.L. Zhang, J.L. Meng, L. Guo, and Z.C. Guo, Numerical study of the reduction process in an oxygen blast furnace, *Metall. Mater. Trans. B*, 47(2016), No. 1, p. 467.

[4] W.Q. Xu, W.J. Cao, T.Y. Zhu, Y.J. Li, and B. Wan, Material flow analysis of CO_2 emissions from blast furnace and basic oxygen furnace steelmaking systems in China, *Steel Res. Int.*, 86(2015), No. 9, p. 1063.

[5] J. Tang, M.S. Chu, F. Li, C. Feng, Z.G. Liu, and Y.S. Zhou, Development and progress on hydrogen metallurgy, *Int. J. Miner. Metall. Mater.*, 27(2020), No. 6, p. 713.

[6] M. Naito, A. Okamoto, K. Yamaguchi, T. Yamaguchi, and Y. Inoue, Improvement of blast furnace reaction efficiency by use of high reactivity coke, *Tetsu-to-Hagané*, 87(2001), No. 5, p. 357.

[7] M. Naito, A. Okamoto, K. Yamaguchi, T. Yamaguchi, and Y. Inoue, Improvement of blast furnace reaction efficiency by temperature control of thermal reserve zone, *Nippon Steel Tech. Rep.*, 2006, No. 94, p. 103.

[8] S. Nomura, K. Higuchi, K. Kunitomo, and M. Naito, Reaction behavior of formed iron coke and its effect on decreasing thermal reserve zone temperature in blast furnace, *ISIJ Int.*, 50(2010), No. 10, p. 1388.

[9] M. Naito, S. Nomura, and K. Kato, Development of production and utilization technology of coke with high strength and high reactivity, *Tetsu-to-Hagané*, 96(2010), No. 5, p. 17.

[10] S. Nomura, H. Terashima, E. Sato, and M. Naito, Some fundamental aspects of highly reactive iron coke production, *ISIJ Int.*, 47(2007), No. 6, p. 823.

[11] T. Anyashiki, H. Fujimoto, T. Yamamoto, T. Sato, H. Matsuno, M. Sato, and K. Takeda, Basic examination of briquetting technology for ferro-coke process on 0.5 t/d bench scale plant, *Tetsu-to-Hagané*, 101(2015), No. 10, p. 515.

[12] H.T. Wang, M.S. Chu, W. Zhao, R. Wang, Z.G. Liu, and J. Tang, Fundamental research on iron coke hot briquette − a new type burden used in blast furnace, *Ironmaking Steelmaking*, 43(2016), No. 8, p. 571.

[13] H.T. Wang, W. Zhao, M.S. Chu, Z.G. Liu, J. Tang, and Z.W. Ying, Effects of coal and iron ore blending on metallurgical properties of iron coke hot briquette, *Powder Technol.*,

328(2018), p. 318.
[14] A. Uchida, Y.Yamazaki, S. Matsuo, Y. Saito, Y. Matsushita, H. Aoki, and M. Hamaguchi, Effect of iron ore reduction on ferro-coke strength with hyper-coal addition, *ISIJ Int.*, 105(2016), No. 12, p. 2132.
[15] K. Nishioka, Y. Ujisawa, and T. Inada, Effect of large quantity of ferrocoke charging on reduction of reducing agent rate of blast furnace, *Tetsu-to-Hagané*, 100(2014), No. 11, p. 1347.
[16] S.Z. Shi, Q. Zheng, X.G. Bi, Y.G. Mao, G.E. Wang, and Y.H. Luo, Model-based ferro-coke strength prediction and analysis of its control measures, *J. Taiyuan Univ. Technol.*, 48(2017), No. 1, p. 36.
[17] E. Hosseini, F. Rashchi, and A. Ataie, Ti leaching from activated ilmenite-Fe mixture at different milling energy levels, *Int. J. Miner. Metall. Mater.*, 25(2018), No. 11, p. 1263.
[18] N. Vieceli, C.A. Nogueira, M.F.C. Pereira, F.O. Durao, C. Guimaraes, and F. Margarido, Optimization of an innovative approach involving mechanical activation and acid digestion for the extraction of lithium from lepidolite, *Int. J. Miner. Metall. Mater.*, 25(2018), No. 1, p. 11.
[19] Y.T. Wang, S.L. Jiang, H.L. Wang, and H.Y. Bie, A mucoadhesive, thermoreversible *in situ* nasal gel of geniposide for neurodegenerative diseases, *Plos One*, 12(2017), No. 12, p. 1.
[20] Z.J. Yang, K.K. Wang, and Y. Yang, Optimization of ECAP−RAP process for preparing semisolid billet of 6061 aluminum alloy, *Int. J. Miner. Metall. Mater.*, 27(2020), No. 6, p. 792.
[21] M. Mondal, A. Ghosh, K. Gayen, G. Halder, and O.N. Tiwari, Carbon dioxide bio-fixation by *Chlorella* sp. BTA 9031 towards biomass and lipid production: Optimization using Central Composite Design approach, *J. CO_2 Util.*, 22(2017), p. 317.
[22] L. Kun, L.L. Zhang, L. Wei, C.S. Okinda, and M.X. Shen, Optimization of compression formulation and load of food-grade tracers for grain traceability using central composite design, *Int. J. Agric. Biol. Eng.*, 10(2017), No. 6, p. 221.
[23] M.D. Turan, Optimization of selective copper extraction from chalcopyrite concentrate in presence of ammonium persulfate and ammonium hydroxide, *Int. J. Miner. Metall. Mater.*, 26(2019), No. 8, p. 946.
[24] S.N.A.M. Hassan, M.A.M. Ishak, and K. Ismail, Optimizing the physical parameters to achieve maximum products from co-liquefaction using response surface methodology, *Fuel*, 207(2017), p. 102.
[25] D. Singh, P.M. Pandey, and D. Kalyanasundaram, Optimization of pressure-less microwave sintering of Ti6Al4V by response surface methodology, *Mater. Manuf. Process.*, 33(2018), No. 16, p. 1835.
[26] China National Standardization Administration Committee, Chinese National Standard GB/T 4000-2017: *Determination of Coke Reactivity Index (CRI) and Coke Strength after Reaction (CSR)*, Standards Press of China, 2017.
[27] S.K. Singh, P. Singha, and K. Muthukumarappan, Modeling and optimizing the effect of extrusion processing parameters on nutritional properties of soy white flakes-based extrudates using response surface methodology, *Anim. Feed. Sci. Technol.*, 254(2019), art. No. 114197.
[28] S. Kim, S.C. Ko, Y.S. Kim, S.K. Ha, H.Y. Park, Y. Park, and S.H. Lee, Determination of *Curcuma longa* L. (Turmeric) leaf extraction conditions using response surface methodology to optimize extraction yield and antioxidant content, *J. Food Quality*, 2019(2019), p. 1.
[29] X.R. Zhang, Z.H. Liu, X. Fan, X. Lian, and C.Y. Tao, Optimization of reaction conditions for the electroleaching of manganese from low-grade pyrolusite, *Int. J. Miner. Metall. Mater.*, 22(2015), No. 11, p. 1121.
[30] J.Jiang, Y.P. Chen, J.Z. Cao, and C.T. Mei, Improved hydrophobicity and dimensional stability of wood treated with paraffin/acrylate compound emulsion through response surface methodology optimization, *Polymers*, 12(2020), No. 1, art. No. 86.
[31] B.D. Flores, A. Guerrero, I.V. Flores, A.G. Borrego, M.A. Diez, E. Osorio, and A.C.F. Vilela, On the reduction behavior, structural and mechanical features of iron ore-carbon briquettes, *Fuel Process. Technol.*, 155(2017), p. 238.
[32] China National Standardization Administration Committee, Chinese National Standard GB/T 1996—2017: *Coke for Metallurgy*, Standards Press of China, 2017.